JOURNAL OF MATERIALS SCIENCE 30 (1995) 1321–1326

Sintering and compensation effect of donor and acceptor codoped 3 mol % Y_2O_3–ZrO_2

SAN-YUAN CHEN
Department of Materials Science and Engineering, The University of Michigan, Ann Arbor, MI 48019, USA

HONG-YANG LU
Institute of Materials Science and Engineering, National Sun Yat-Sen University, Kaohsiung 80424, Taiwan

Addition of 0.15–0.5 mol % acceptor oxide, Al_2O_3, to 3 mol % Y_2O_3–ZrO_2 results in enhanced densification at 1350 °C. The enhancement is accounted for by a liquid phase sintering mechanism. While the addition of donor oxide, Ta_2O_5, of 0.15–2.5 mol % at 1300–1600 °C results in the decrease of final density and in the destabilization of the tetragonal (t) phase of the 3 mol % Y_2O_3–t-ZrO_2 (TZP). X-ray diffractometry (XRD) reveals that the Ta_2O_5–added 3 mol % Y_2O_3–ZrO_2 contains monoclinic (m) ZrO_2 phase and a second $Ta_2Zr_6O_{17}$ phase. The decrease is attributed to the increase of m-ZrO_2 content in these samples. Complete phase transformation from t-ZrO_2 to m-ZrO_2 observed in samples added with 2.5 mol % Ta_2O_5 is interpreted by the compensation effect based on donor and acceptor codoping defect chemistry.

1. Introduction

Minor addition of Al_2O_3 was found to enhance densification of Y_2O_3 stabilized ZrO_2 compositions [1–5]. A liquid phase sintering mechanism [2, 3] was proposed to account for the enhancement. While addition of this liquid residue to grain boundaries after cooling to room temperature was the major cause for assisting densification, grain boundary pinning of the Al_2O_3 inclusions was also responsible for the densification improvement [3]. Nevertheless, mass transport increase via a doping mechanism [3], due to limited solid solution of $-$ 0.1 mol % Al_2O_3 in ZrO_2 [5], has also been reported to assist the densification of the ceramic. A maximum bending strength of 2380 MPa at 20 wt % Al_2O_3 addition was reported for 3 mol % Y_2O_3–ZrO_2 [6] when this powder was hipped (hot isostatic pressed). By pressureless sintering, the maximum flexural strength was again obtained from 7.5 mol % Y_2O_3–ZrO_2 added with 20 wt % Al_2O_3; however, the maximum flexural strength dropped to 460 MPa [7].

Taking the terminology of donor and acceptor as normally used in semiconductors, Ta^{+5}, a donor ion, when substituted in the Zr^{+4} site, gives up an electron and forms a positively charged defect, Ta'_{zr}; and Al^{+3} an acceptor ion, when substituted in the Zr^{+4} site, accepts an electron and results in a negatively charged defect Al'_{zr}. The addition of Ta_2O_5 to Y_2O_3–ZrO_2 compositions led to a decrease of the critical grain size for the tetragonal (t) to monoclinic (m) phase transformation, reported by Kim and Tien [8]. The transformation of t-ZrO_2 to m-ZrO_2 was [8] further related to an increase in the c/a ratio of Y_2O_3–TZP; the fracture toughness increased from 4.5 to 12 MPa $m^{1/2}$ in their studies [8] of ZrO_2–Y_2O_3–Ta_2O_5.

Reported here is the sintering behaviour of an acceptor (3 mol % Y_2O_3) doped ZrO_2 when acceptor oxide Al_2O_3 and donor oxide Ta_2O_5 are added, respectively. A possible mechanism of densification enhancement is discussed, and the compensation effect due to the donor and acceptor codoping is explained.

2. Experimental procedure

A 3 mol % Y_2O_3–ZrO_2 (TZ3Y Toyo Soda, Japan) powder containing trace impurities of 100 p.p.m. SiO_2, 20 p.p.m. Fe_2O_3 and 70 p.p.m. Na_2O was used in this study. The powder was mixed with an appropriate quantity of 0.05–5.0 mol % Al_2O_3 powder (AKP-50 Sumitomo, Japan) in a high purity ($> 99.9\%$) Al_2O_3 ball mill with 3 mol % Y_2O_3–ZrO_2 balls, using deionized water medium. This was followed by oven drying at 110 °C. Ta_2O_5 (Merck, FRG) of 0.15–5.0 mol % was added in oxide form to TZ3Y powder and then followed by the same procedures of ball-milling and drying. The powder was deagglomerated using an agate mortar and pestle before being dry pressed to discs of 12 mm diameter in a (Tungster Carbide) WC-inserted steel die at a pressure of 100 MPa. These discs were then sintered at temperatures of 1250–1600 °C for 2–12 h. Relative density was measured by the Archimedes' method, using deionized water as a dispersing agent. Sintered samples were then mechanically ground to 30 μm before being lapped from 12 to 1 μm surface roughness with diamond paste, successively. For transmission

0022–2461

electron microscopy (TEM) observation, these lapped samples were then dimpled before being Ar^+ ion beam thinned to electron transparency. Scanning electron microscopy (SEM, Camscan, England) coupled with energy dispersive X-ray (EDX) analysis (Kevex, USA) and TEM (Jeol 2000FX, Japan) were used for microstructural analysis. Grain size was determined by the lineal intercept method, as described by Mendelson [9]. Crystalline phases were identified by a Philips PW1820 diffractometer with CuK_α radiation operating at 40 kV, 30 mV. The phase content of ZrO_2 was determined by X-ray diffraction (XRD) following the technique developed by Garvie and Nicholson [10].

3. Results

3.1. Effect of Al_2O_3 addition

3.1.1. General

A relative final density, ρ_{rel}, of 99.7% theoretical density (TD) was obtained when 0.15–0.5 mol % Al_2O_3 added powder was sintered at 1350–1400 °C for 2 h (Fig. 1a). When the sintering temperature was raised to 1500–1600 °C, the same range of dopant concentration, however, resulted in lower final densities (Fig. 1b) compared to those in Fig. 1a. The sintering temperature was reduced from 1500 °C (Fig. 1b) to 1350 °C

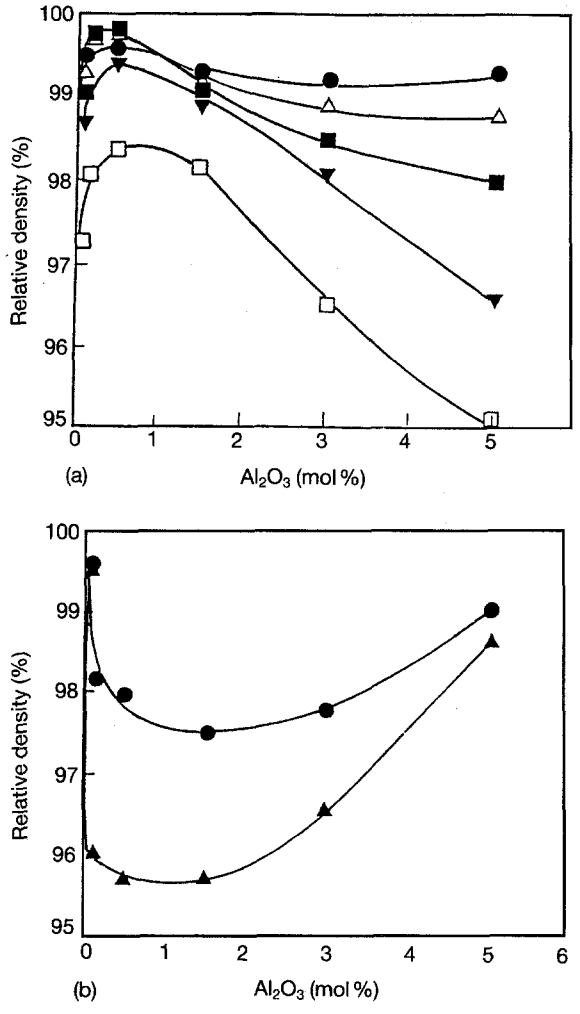

Figure 1 Relative final density of Al_2O_3 added 3 mol % Y_2O_3–ZrO_2 when sintered at (a) (●) 1450 °C, (△) 1400 °C, (■) 1350 °C, (▼) 1300 °C, (□) 1250 °C 2 h^{-1}; and (b) (●) 1500 °C, (▲) 1600 °C 2 h^{-1}.

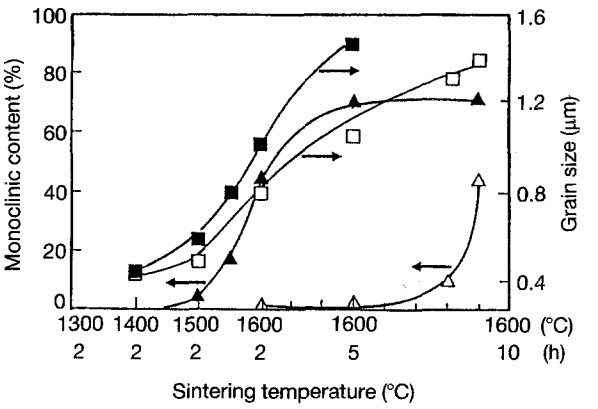

Figure 2 Increase of m-ZrO_2 content and average grain size for the (△, □) unaltered YTZP 0.5 mol % Al_2O_3 added (▲, ■) when sintered at 1200–1600 °C.

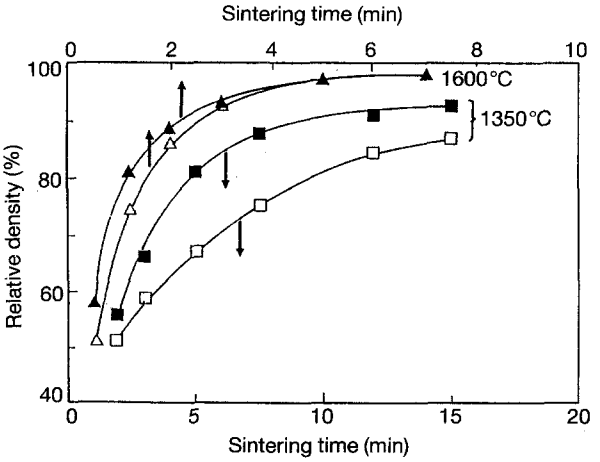

Figure 3 Densification enhancement by Al_2O_3 addition in the intermediate stage of sintering: (△, □) unaltered YTZP; (▲, ■) 0.5 mol % Al_2O_3–YTZP.

with Al_2O_3 addition of 0.15–0.5 mol %, while sustaining a comparable relative final density of 99.7% TD.

The m-ZrO_2 phase content increased progressively from less than 10% in 0.5 mol % Al_2O_3 added 3 mol % Y_2O_3–ZrO_2 samples sintered at 1300 °C to 60% when the sintering temperature was raised to 1600 °C (Fig. 2). For those of the unadded 3 mol % Y_2O_3–ZrO_2 samples, even with prolonged heating of 9 h at 1600 °C, the amount of m-ZrO_2 phase still remained 50%. While for the addition of Al_2O_3 at 0.5 mol %, the m-ZrO_2 content was found to increase with both sintering temperature and time. The critical grain size, G_{crit}, for the t–m transformation is taken as the average grain size when 5% m-ZrO_2 was detected by XRD. This G_{crit} (Fig. 2) decreased from 1.30 μm [8] unadded to 0.60 μm for 0.5 mol % Al_2O_3 added 3 mol % Y_2O_3–ZrO_2 samples.

3.1.2. Densification

Densification enhancement by adding Al_2O_3 is best evidenced in 0.5 mol % Al_2O_3 added 3 mol % Y_2O_3–ZrO_2 (Fig. 3), sintered at a temperature of 1350 °C. A relative final density of 90% TD obtained within 10 min of sintering at 1350 °C was better than

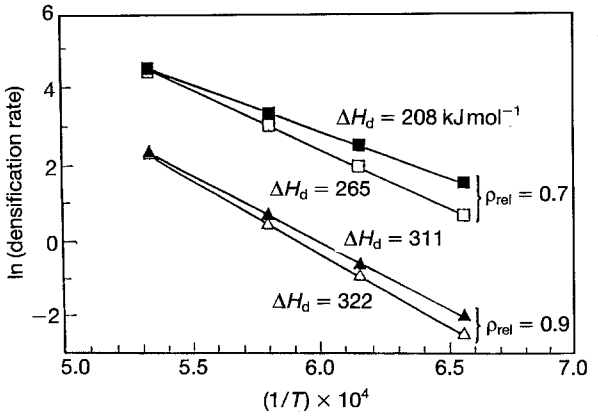

Figure 4 Activation enthalpy for the Al_2O_3 added 3 mol % Y_2O_3–ZrO_2 and the unadded: (□, △) unaltered YTZP; (▲, ■) 0.5 mol % Al_2O_3–YTZP.

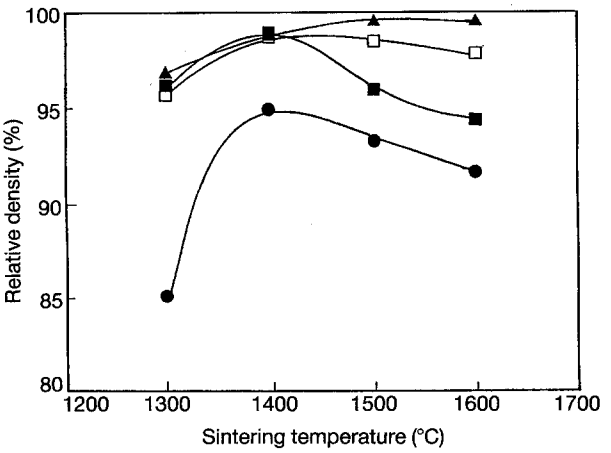

Figure 5 Relative final density of Ta_2O_5 added 3 mol % Y_2O_3–ZrO_2 when sintered at 1300–1600 °C 2 h^{-1}: (▲) $x = 0$, (□) $x = 0.0015$, (■) $x = 0.01$, (●) $x = 0.025$.

only 80% TD of the unadded. The enhancement effect was comparatively less significant when samples were sintered at the higher temperature of 1600 °C. The densification rate of a ceramic powder compact is taken as the first derivative of the densification curve, described by plotting the relative final density versus sintering time. The densification rate at a particular relative final density was then obtained by drawing the tangent to the densification curve for the corresponding ρ_{rel}, e.g. $\rho_{rel} = 0.6$, 0.7 and 0.9 as shown in Fig. 4. The densification curves for the 0.5 mol % Al_2O_3 added 3 mol % Y_2O_3–ZrO_2 are given in Fig. 3 for sintering at 1350 and 1600 °C, respectively. The densification enthalpy, ΔH_d was obtained by plotting the logarithm of densification rate, ln (d ρ/dt), against the reciprocal temperature, $1/T$, as shown in Fig. 4.

3.1.3. Microstructural features

The unadded 3 mol % Y_2O_3–ZrO_2 powder yielded a homogeneous microstructure of average grain size 1 μm, similar to that observed in previous studies [11, 12]. Added with Al_2O_3 gave a typical microstructure of bimodal grain size distribution, which was also similar to the MgO added 3 mol % Y_2O_3–ZrO_2 [12]. Normally, residual porosity and intergranular cracks were observed in the Al_2O_3 added samples. For those with 0.5 mol % Al_2O_3 addition and sintered at 1600 °C 5 h^1, large grains exhibited the typical t + c "tweed" contrast [13] on TEM, which has grown at the expense of surrounding small grains by a coalescence mechanism [12].

3.2. Effect of Ta_2O_5 addition

3.2.1. General

There is no significant decrease in the final density of 3 mol % Y_2O_3–ZrO_2 from minor Ta_2O_5 addition of 0.15 and 1.0 mol %. However, for higher sintering temperatures, i.e. 1500 and 1600 °C (Fig. 5), the relative final density decreases with higher sintering temperature, and also with higher Ta_2O_5 addition. The optimal relative final density of 99.0% TD obtained

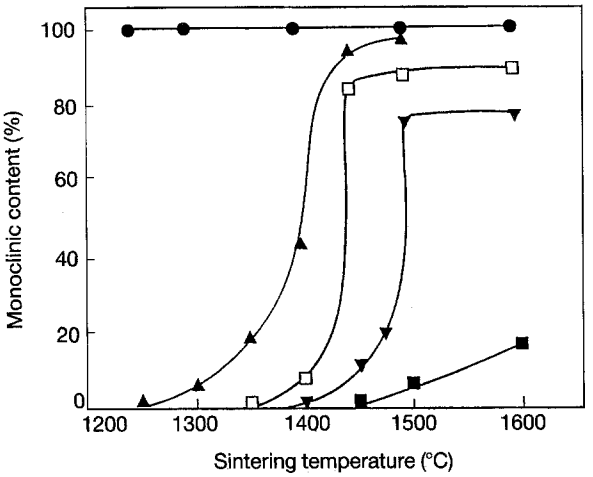

Figure 6 Increase of m–ZrO_2 content with Ta_2O_5 addition and sintering temperature: (■) $x = 0.015$, (▼) $x = 0.005$, (●) $x = 0.025$, (▲) $x = 0.015$, (□) $x = 0.01$.

with 1.0 mol % Ta_2O_5 addition at a sintering temperature of 1400 °C, is lower than that of the unadded (99.6% at 1500 °C). For sintering at 1600 °C, the relative final density dropped from 99.5% TD of the unadded to 92% TD of the 2.5 mol % added 3 mol % Y_2O_3–ZrO_2 samples.

3.2.2. Critical grain size for transformation

The m-ZrO_2 content increased with sintering temperature and with the level of Ta_2O_5 addition (Fig. 6). Taking 5% transformation from t-ZrO_2 to m-ZrO_2 as an indication, when sintered for 2 h, m-ZrO_2 started to emerge at a lower temperature for higher Ta_2O_5 addition, e.g. 1300 °C, 1.5 mol % versus 1500 °C, 0.15 mol %. When the addition of Ta_2O_5 amounted to 2.5 mol %, the sample yielded 100% m-ZrO_2 phase for sintering temperatures of 1250–1600 °C. The G_{crit} for the t–m transformation dropped sharply from 1.30 to 0.55 μm with only 0.15 mol % Ta_2O_5 addition to 3 mol % Y_2O_3–ZrO_2. When Ta_2O_5 was further increased, G_{crit} gradually levelled off at 0.45 μm (Fig. 7).

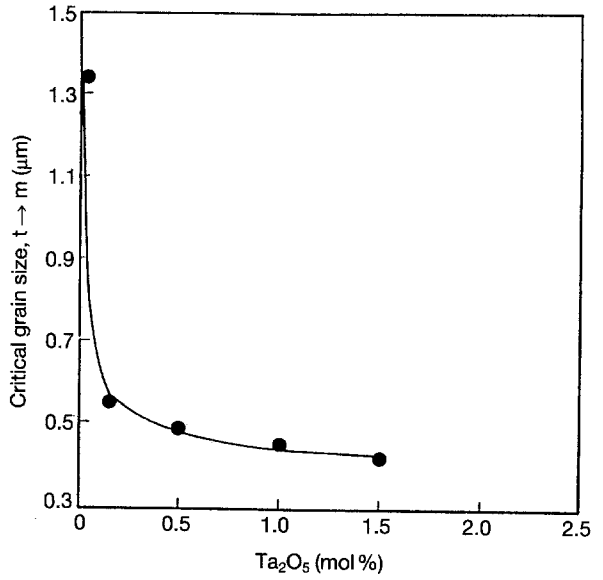

Figure 7 Critical grain size for t–m transformation when Ta_2O_5 added to 3 mol % Y_2O_3–ZrO_2.

3.2.3. Microstructural features

Ta_2O_5 added samples sintered at 1500 °C for 2 h having dispersed porosity and an average grain size of 1 μm, were poorly densified. Cracks were also found when the addition of Ta_2O_5 was less than 2.5 mol %. The increase of Ta_2O_5 addition to 5.0 mol %, however, resulted in larger ZrO_2 grains with dispersed second phases located either intergranularly on in triple junctions. Some grains (not shown here) exhibiting the surface relief upheaval on SEM microstructure are characteristic of the transformed m-ZrO_2 phase [14] resulting from the t–m martensitic phase transformation; intergranular cracks found adjacent to the transformed ZrO_2 grain are consistent with transformation accompanied volume expansion. When the addition of Ta_2O_5 was 1.0 mol %, TEM observation revealed no second phase of glassy nature, while the crystalline second phase containing Ta^{+5}, as confirmed by EDAX analysis, was ubiquitous. XRD identified the second phase as the $Ta_2Zr_6O_{17}$ compound.

4. Discussion

4.1. Liquid phase sintering

Densification enhancement by 0.15–0.5 mol % addition of Al_2O_3 can be attributed to the formation of a liquid at the sintering temperature, as previously proposed [1, 2]. Enhancement at 1350 °C, with only 0.5 mol % Al_2O_3 addition, occurred at the intermediate stage of the sintering process (< 90% TD) (Fig. 3). In the case of Ta_2O_5 addition, formation of extensive solid solutions occurred between the SiO_2 trace impurity, associated with the starting powder, and the Ta_2O_5 dopant in the Ta_2O_5-rich part of the SiO_2–Ta_2O_5 binary phase diagram [15]. The binary eutectic only formed in the SiO_2-rich part at 1570 °C. Liquid therefore was expected to play a minor role in affecting densification at sintering temperatures < 1570 °C. TEM observations, revealing no glassy grain boundary phase, support this argument.

ΔH_d is the activation enthalpy of a combination of atom migration processes. In the intermediate stage, a lower ΔH_d value (208 versus 265 kJ mol^{-1}) indicates liquid assisted densification due to the addition of Al_2O_3 (Fig. 4). As densification proceeds to 90% TD, the solid state sintering mechanism becomes predominant for both the added and the unadded Al_2O_3, and ΔH_d approximates to a similar value.

4.2. Defect chemistry and densification by the solid state mechanism

The addition of 0.15–0.5 mol % Al_2O_3 resulted both in enhancing the densification at 1350 °C (Fig. 1a) and in hampering densification at 1600 °C (Fig. 1b). A sharp decline of the relative final density (Fig. 1b), particularly at higher Al_2O_3 addition, can be accounted for by the increasing content of m-ZrO_2, which amounted to 50% for 0.5 mol % Al_2O_3 addition (Fig. 2) sintered at 1600 °C 2 h[1].

Y_2O_3, added to ZrO_2 to stabilize the high temperature cubic (c) and tetragonal (t) phases, is an acceptor oxide for ZrO_2. Discussion of the stabilization mechanism of the c or t phase when solute oxides, such as MgO or Y_2O_3, are added to ZrO_2 indicated [16] that an oxygen vacancy thus created played an important role in the stabilization. Al_2O_3, as well as Y_2O_3, is an acceptor oxide to ZrO_2. Within the solid solubility of 0.1 mol % at 1300 °C [5], its dissolution to the c-ZrO_2 lattice occupies the Zr^{+4} site. Supposing that the intrinsic defect is the Schottky type, and $V_O\cdot\cdot$ is the principal compensating defect, dissolution creates an equivalent molar quantity of oxygen vacancy, $V_O\cdot\cdot$, via defect reaction. The defect reaction equation can then be written as

$$Al_2O_3 \longrightarrow 2Al'_{Zr} + V_O\cdot\cdot + 3O_O^x$$

The formation of $V_O\cdot\cdot$ will supplement the already existing $V_O\cdot\cdot$ due to the addition of Y_2O_3. In solid state sintering, however, the slowest moving ion along its fastest path controls the densification rate [17]. The Zr^{+4} cation lattice diffusion with the diffusion coefficient D^L_{Zr}, and cation interstitials, $Zr_i\cdot\cdot\cdot\cdot$, were considered to be the rate determining step and species [18], respectively. Thus the formation of $V_O\cdot\cdot$ by the additional acceptor, Al_2O_3, could effect the densification in the reverse direction, i.e. hampering rather than enhancing.

In the extrinsic region, where the Frenkel type of defect predominates, as the content of Al_2O_3 acceptor dopant increases, it is assumed that $[Al'_{Zr}] > [V_O\cdot\cdot]$ and e′ and h· are neglected for convenience. The neutrality approximation

$$(Al'_{Zr}) + 4(V''_{Zr}) + 2(O''_i) + e' = h\cdot + 2(V_O\cdot\cdot) + 4(Zr_i\cdot\cdot\cdot\cdot)$$

becomes

$$(Al'_{Zr}) = 4(Zr_i\cdot\cdot\cdot\cdot)$$

The straight line repersenting $(Zr_i\cdot\cdot\cdot\cdot)$ runs in parallel to the line representing the concentration of the

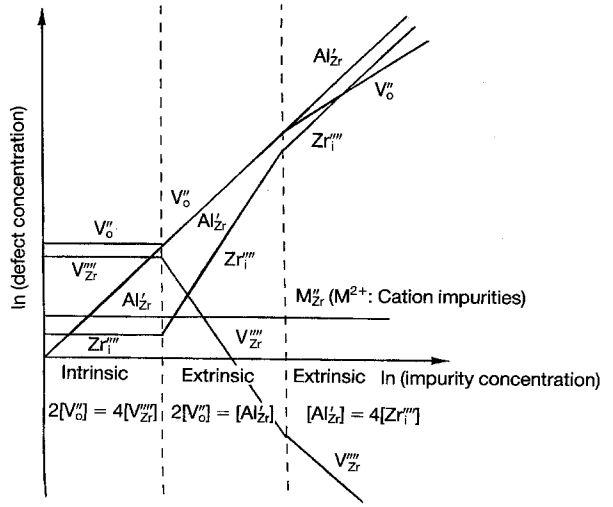

Figure 8 Brouwer defect equilibrium diagram for addition of Al_2O_3 to ZrO_2.

substitutional defect, $[Al'_{Zr}]$, having a slope of unity in the Brouwer defect equilibrium diagram (Fig. 8). That is to say, $Zr_i \cdot \cdot \cdot \cdot$ increases in direct proportion to the concentration of the Al_2O_3 acceptor dopant. On the other hand, $V_O \cdot \cdot$ will also increase, but at a slower rate of slope of 1/2. Therefore, it is likely that at lower sintering temperatures, the enhancement of densification is mainly due to the liquid assisted mechanism. As the sintering temperature is raised, solubility of Al_2O_3 in ZrO_2 is increased, and the ceramic exhibits extrinsic behaviour, such that the principal compensating defect, i.e. $Zr_i \cdot \cdot \cdot \cdot$, increases. Consequently, the densification is further augmented by a solid state sintering mechanism when D^L_{Zr}; lattice diffusion through Zr-interstitials is encouraged. In fact, the relative final density has indeed raised at 0.5 mol % Al_2O_3 addition; and it becomes progressively evident when the temperature is increased from 1250 to 1450 °C (Fig. 1a).

As the sintering temperature is raised still higher to 1600 °C, further increase of Al_2O_3 solubility in ZrO_2 is expected; more Al_2O_3 is allowed to dissolve into the ZrO_2 lattice; and the lattice diffusion process, D^L_{Zr}, having higher activation enthalpy [17] is preferentially encouraged relative to the surface diffusion process. The densification–coarsening ratio [17] is thus improved to favour the densification. When the sintering temperature is raised to 1600 °C, 0.5 mol % Al_2O_3 addition experienced on almost identical degree of densification in the intermediate stage of sintering as that of the unadded sample (Fig. 3). The neutrality approximation in this extrinsic region, where $(Al'_{Zr}) > (V''''_{Zr})$, is written as

$$(Al'_{Zr}) = 2(V_O \cdot \cdot)$$

where $V_O \cdot \cdot$ is the predominant defect species which may again affect the densification reversely (Fig. 1b). Moreover, due to this hinderance and the higher content of m-ZrO_2, the relative final density experienced a trough at 1.0 mol % Al_2O_3 addition (Fig. 1b). When the Al_2O_3 content increases from 1.0 mol % to the extent (5 mol %) that the ceramic exhibits extrinsic behaviour and $[Al'_{Zr}] = 4(Zr_i \cdot \cdot \cdot \cdot)$, where the cationic interstitial, $Zr_i \cdot \cdot \cdot \cdot$, responsible for the densification enhancement predominates an increase of the relative final density results (Fig. 1b).

If the intrinsic disorder is of the Schottky type, addition of Ta_2O_5 results in the formation of the substitutional defect, Ta'_{Zr}, and cationic vacancies, V''''_{Zr}, via the defect reaction equation

$$2\,Ta_2O_5 \longrightarrow 4\,Ta'_{Zr} + V''''_{Zr} + 10O^x_O$$

while Y_2O_3 addition created Y'_{Zr} and $V_O \cdot \cdot$ by

$$Y_2O_3 \longrightarrow 2\,Y'_{Zr} + V_O \cdot \cdot + 3O^x_O$$

Although D^L_{Zr}, Zr^{+4} cationic lattice diffusion may have been encouraged by the increased V''''_{Zr} due to Ta_2O_5 addition; decrease of the relative final density mainly due to the increased m-ZrO_2 content, the lower TD of m-ZrO_2 compared to that of t-ZrO_2, has overwhelmed the densification enhancement by the solid state mechanism (Fig. 6). An example is seen in the 0.5 mol % Ta_2O_5 addition which was sintered at 1500 °C yielding 80% m-ZrO_2, and resulted in 96.4% TD.

4.3. Compensation effect

Grain growth inhibition resulting from MgO addition in the Al_2O_3 ceramic could be counteracted by codoping with ZrO_2 of equimolar quantity [19]. The compensation effect resulting in the counteraction of semiconductivity, was proposed previously for donor and acceptor codoped semiconducting $BaTiO_3$ [20]. Defect compensation as a controlling factor of abnormal grain growth in $BaTiO_3$ was also reported by Brook et al. [21], and room temperature resistivity was restored [20, 22] in the donor doped $BaTiO_3$ by adding half the molar quantity of the acceptor.

For the donor (Ta_2O_5) and acceptor (Y_2O_3) codoped ZrO_2, the neutrality approximation can be written as follows

$$(Ta'_{Zr}) + 2(V_O \cdot \cdot) = (Y'_{Zr}) + 4(V''''_{Zr})$$

This neutrality approximation predicts that the defect concentration due to acceptor substitution $[Y'_{Zr}]$, increases with that created by the donor dopant, $[Ta_{Zr} \cdot]$ by a slope of unity, i.e. a direct proportional relationship. Both the decrease of the critical grain size for the t–m transformation and the emergence of m-ZrO_2 when Ta_2O_5 is added (Figs 6 and 7), indicate that Ta_2O_5 donor codoping leads to the destabilization of t-ZrO_2. In fact, following sintering at 1250–1600 °C, when the addition of Ta_2O_5 reaches a level of 2.5 mol %, the 3 mol % Y_2O_3–TZP (tetragonal ZrO_2 polycrystals) completely transforms to m-ZrO_2 (Fig. 6). The high temperature phase, t-ZrO_2 is stabilized and retained at room temperature as bulk TZP by the addition of 3 mol % Y_2O_3 acceptor. Neutrality is maintained as long as $(Ta'_{Zr}) - (Y'_{Zr}) = 0$, where acceptor and donor are compensated completely. Therefore, when an equal molar quantity of donor, i.e. Ta^{+5} is codoped, the destabilization of t-ZrO_2 by Y_2O_3 addition is then counteracted. It is expected

from the neutrality approximation that t-ZrO_2 is destabilized and m-ZrO_2 is completely restored. In fact, the approximate equality (2.5 and 3.0) of the molar quantity of donor and acceptor oxide in this study, suggests that the compensation effect induced by Ta_2O_5 donor codoping is to counteract t-ZrO_2 stabilization due to Y_2O_3 acceptor addition.

5. Conclusions

1. Addition of Al_2O_3 acceptor oxide to 3 mol % Y_2O_3–ZrO_2 enhanced sintering by a liquid assisted densification mechanism at 1350 °C.

2. Addition of Ta_2O_5 donor oxide to 3 mol % Y_2O_3–ZrO_2 hampered densification and destabilized the t-ZrO_2.

3. The complete transformation of t-ZrO_2 to m-ZrO_2, when added with 2.5 mol % Ta_2O_5 to 3 mol % Y_2O_3–ZrO_2, was explained by a compensation effect based on defect chemistry.

References

1. K. C. RADFORD and R. J. BRATTON, *J. Mater. Sci.* **14** (1979) 59.
2. R. C. BUCHANAN and D. M. WILSON, in "Advances in Ceramics", Vol. 10, edited by W. D. Kingrey (American Ceramic Society, Columbus, OH, 1984) pp. 526–540.
3. E. P. BUTLER and J. DRENNAN, *J. Amer. Ceram. Soc.* **65** (1982) 474.
4. W. D. TOUHIG and T. Y. TIEN, *ibid.* **63** (1980) 595.
5. H. BERNARD, PhD thesis, University of Grenoble, France, 1981
6. K. TSUKUMA, M. SHIMADA and K. UEDA, *J. Amer. Ceram. Soc.* **68** (1985) C-4.
7. F. J. ESPER, K. H. FRIESE and H. GEIER, in "Advances in Ceramics", Vol. 12, edited by N. Claussen, M. Ruhle and A. H. Heuer (American Ceramic Society, Columbus, OH, (1984) pp. 528–536.
8. D. J. KIM and T. Y. TIEN, "Effect of Ta_2O_5 Alloying on the Transformability of Y-TZP", American Ceramic Society 89th Annual Meeting, 126-B-87 (Columbus, OH, 1987).
9. M. I. MENDELSON, *J. Amer. Ceram. Soc.* **55** (1972) 303.
10. R. C. GARVIE and P. S. NICHOLSON, *ibid.* **55** (1969) 443.
11. H. Y. LU and S. Y. CHEN, *ibid.* **70** (1987) 537.
12. H. Y. LU and J. S. BOW, *ibid.* **72** (1989) 228.
13. R. H. J. HANNINK, *J. Mater. Sci.* **13** (1978) 2487.
14. G. K. BANSAL and A. H. HEUER, *Acta Metall.* **20** (1972) 1281.
15. "Phase Diagrams for Ceramist-1975 Supplement", (American Ceramic Society, Columbus, OH, 1975) Figs 4447 and 4448.
16. M. MORINAGA, H. ADACHI and M. TSUKUDA, *J. Phys. Chem. Solids* **44** (1983) 301.
17. R. J. BROOK, *Proc. Brit. Ceram. Soc.* **32** (1982) 7.
18. S. WU and R. J. BROOK, *Solid State Ionics* **14** (1984) 123.
19. S. J. BENNISON and M. P. HARMER, *J. Amer. Ceram. Soc.* **68** (1985) C-22.
20. C. J. PENG and H. Y. LU, *J. Amer. Ceram. Soc.* **71** (1988) C-44.
21. R. J. BROOK, W. H. TUAN and L. A. XUE, in "Ceramic Transaction - Ceramic Powder Science", edited by G. L. Messing, E. R. Fuller and H. Hausner (American Ceramic Society, Westerville, OH, 1988) pp. 811–823.
22. C. J. TING, C. J. PENG, H. Y. LU and S. T. WU, *J. Amer. Ceram. Soc.* **73** [2] (1990) 329.

Received 30 September 1993
and accepted 6 July 1994